How a moving passive observer can perceive its environment ? The Unruh effect revisited

Mathias Fink, Josselin Garnier

Version of Record: https://www.sciencedirect.com/science/article/pii/S0165212519300150
Manuscript_0a7dc46cf6549565a1e75ccc1459f8ca

How a moving passive observer can perceive its environment ? The Unruh effect revisited

Mathias Fink[a], Josselin Garnier[b]

[a] *Institut Langevin, ESPCI and CNRS, PSL Research University, 1 rue Jussieu, 75005 Paris, France*
[b] *Centre de Mathématiques Appliquées, Ecole polytechnique, 91128 Palaiseau Cedex, France.*
josselin.garnier@polytechnique.edu *(corresponding author).*

Abstract

We consider a point-like observer that moves in a medium illuminated by noise sources with Lorentz-invariant spectrum. We show that the autocorrelation function of the signal recorded by the observer allows it to perceive its environment. More precisely, we consider an observer with constant acceleration (along a Rindler trajectory) and we exploit the recent work on the emergence of the Green's function from the cross correlation of signals transmitted by noise sources. First we recover the result that the signal recorded by the observer has a constant Wigner transform, i.e. a constant local spectrum, when the medium is homogeneous (this is the classical analogue of the Unruh effect). We complete that result by showing that the Rindler trajectory is the only straight-line trajectory that satisfies this property. We also show that, in the presence of an obstacle in the form of an infinite perfect mirror, the Wigner transform is perturbed when the observer comes into the neighborhood of the obstacle. The perturbation makes it possible for the observer to determine its position relative to the obstacle once the entire trajectory has been traversed.

Keywords: Passive imaging, correlation-based imaging, noise sources, moving sensors, Unruh effect, Rindler trajectory.

Highlights:

- Analysis of the signal recorded by a moving observer illuminated by noise sources.
- Identification of the trajectories for which the Wigner transform is stationary.
- Characterization of the perturbation of the Wigner transform due to an obstacle.

Declarations of interest: none

1. Introduction

It has been shown that the cross correlations of the signals recorded by a stationary receiver array and transmitted by opportunistic or ambient noise sources can be used to image the environment of the array [12, 14]. It is possible to estimate travel times between receivers in order to estimate the background velocity tomographically [23] or to detect and localize reflectors in the medium [15]. These ideas have been exploited in particular in seismology [8, 25] and they require the use of arrays or networks of sensors. Indeed, the autocorrelation function of the signal recorded by a unique stationary point-like receiver contains little information about its environment. We will see that a stationary receiver or observer can, however, estimate its distance from an obstacle but nothing more.

The situation is different when the observer is moving, because the observer may then be able to exploit the synthetic aperture generated by its trajectory. For instance, active synthetic aperture radar (when the moving antenna transmits and receives) has proved to be a very efficient imaging modality [5, 7] and bistatic or passive versions (when the moving antenna only records and uses signals transmitted by controlled or opportunistic sources) are now the subject of intense research [2, 11, 13, 20]. When the observer is moving, the autocorrelation function of the recorded signal depends in a complicated and interesting way of the environment. In [10] the situation in which a receiver is moving along a circular trajectory is addressed. It is shown that the autocorrelation function of the recorded signal is related to the matrix of Green's function between pairs of points along the trajectory, more exactly to a diagonal band of this matrix whose thickness is determined by the velocity of the receiver. As an application, when a point-like reflector is present within the circular trajectory of the receiver, it is shown how to use the autocorrelation function of the recorded signal to localize the reflector by migration. The processing is, however, quite complex, because it requires to extract the components of the correlation function due to the reflector. It would be of great interest to determine and study a trajectory for which the unperturbed autocorrelation function has a very simple form that makes it possible to detect and identify easily any perturbation.

By investigating the trajectories that would satisfy the desired properties, we have discovered connections with quantum physics and the celebrated Unruh effect. The Unruh effect [24] predicts that an observer along a Rindler trajectory with constant acceleration perceives the quantum vacuum as thermal radiation (i.e. it observes a thermal spectrum of particle excitations). This effect and its applications to black hole radiation and quantum field theory are extensively studied in the literature [17, 6]. Moreover, it is shown to arise from the classical correlation of noise in [3], using a representation of the ambient field as a superposition of incoherent plane waves. In [3] the case of an open medium is addressed, but his approach could be extended to the case of a homogeneous half-space following the decomposition method introduced in [22]. The same approach was used recently in [18] in which the classical analog of the Unruh effect is extensively discussed and a simple experiment on water waves that corroborates the idea is presented. The authors insist on the classical root of the Unruh effect as the correlation of noise in space and time. This work and our own research are, therefore, related, although the motivations are different. We may

say that our paper revisits the pioneering work [3] by using another approach that considers that the ambient field recorded by the observer is generated by noise sources. This gives the same situation as in [3] in a homogeneous medium, but our approach makes it possible to consider the case where the medium is not homogeneous. We demonstrate that the Wigner transform of the field recorded by an observer along a Rindler trajectory is constant when the medium is homogeneous, as originally shown in [3] and observed in [18]. We show in section 2 the original result that the Rindler trajectory is in fact the unique straight-line trajectory that satisfies this property. We finally show that the Wigner transform of the field recorded by a Rindler observer is perturbed by an obstacle when the observer comes into its neighborhood. The perturbation is analyzed in detail in section 3 when the obstacle has the form of an infinite perfect mirror and it is shown that it can be processed to extract the position of the obstacle relative to the observer once the entire trajectory has been traversed.

2. A Rindler observer in a three-dimensional open medium

In this section we show that an observer with a Rindler trajectory is an ideal candidate to probe the environment because the local spectrum of the recorded signal, in the absence of any obstacle, is independent of the position or time along the trajectory. We also show that the Rindler trajectory is, in fact, the unique straight-line trajectory that satisfies this property.

2.1. The noise sources and wave fields

We consider the three-dimensional scalar wave equation for the scalar wave field $u(t, \boldsymbol{x})$ in the full space $\mathbb{R}^3$:

$$\frac{1}{c_o^2}\partial_t^2 u - \Delta u = n(t, \boldsymbol{x}), \tag{1}$$

with radiation condition at infinity. The source term $n(t, \boldsymbol{x})$ models a noise source distribution. It is a zero-mean process, stationary in time and delta-correlated in space:

$$\langle n(t, \boldsymbol{x}) n(t', \boldsymbol{x}') \rangle = F(t - t')\delta(\boldsymbol{x} - \boldsymbol{x}')K(\boldsymbol{x}), \tag{2}$$

where $K(\boldsymbol{x})$ is the function that characterizes the spatial support of the noise source distribution and the Fourier transform $\hat{F}(\omega)$ of $F(t)$ is the power spectral density of the sources.

The analysis of the autocorrelation of the recorded signal follows the lines of the recent work on the emergence of the Green's function from the cross correlation of signals transmitted by noise sources [14]. The covariance function of the wave field has the form

$$\langle u(t, \boldsymbol{x}) u(t', \boldsymbol{x}') \rangle = \frac{1}{2\pi} \int_{\mathbb{R}} \int_{\mathbb{R}^3} \overline{\hat{G}\big(\omega, \boldsymbol{x}, \boldsymbol{y}\big)} \hat{G}\big(\omega, \boldsymbol{x}', \boldsymbol{y}\big) K(\boldsymbol{y}) \hat{F}(\omega) \exp\big[i\omega(t - t')\big] d\boldsymbol{y} d\omega,$$

where $\hat{G}(\omega, \boldsymbol{x}, \boldsymbol{y})$ is the three-dimensional homogeneous Green's function:

$$\hat{G}(\omega, \boldsymbol{x}, \boldsymbol{y}) = \frac{1}{4\pi|\boldsymbol{x} - \boldsymbol{y}|} \exp\Big(i\frac{\omega}{c_o}|\boldsymbol{x} - \boldsymbol{y}|\Big). \tag{3}$$

If we assume that sources are far away, for instance, if the sources are at the surface of a ball with large radius, $K(\boldsymbol{x}) = \delta_{\partial B(\mathbf{0},L)}(\boldsymbol{x})$, then we can invoke Helmholtz-Kirchhoff identity (A.1) and we get

$$\begin{aligned}\langle u(t,\boldsymbol{x})u(t',\boldsymbol{x}')\rangle &= \frac{1}{2\pi}\int_{\mathbb{R}} \frac{c_o}{\omega}\hat{F}(\omega)\mathrm{Im}\hat{G}\big(\omega,\boldsymbol{x},\boldsymbol{x}'\big)\big)\exp\big[i\omega(t-t')\big]d\omega \\ &= \frac{1}{8\pi^2}\int_{\mathbb{R}} \hat{F}(\omega)\mathrm{sinc}\Big(\frac{\omega}{c_o}\big|\boldsymbol{x}-\boldsymbol{x}'\big|\Big)\exp\big[i\omega(t-t')\big]d\omega, \end{aligned} \tag{4}$$

where $\mathrm{sinc}(x) = \sin(x)/x$. This result is in fact very general and holds true for a large class of spatial source distributions, as was shown in the literature about seismic interferometry [8] or ambient noise imaging [14]. From now on we will assume that the spatial distribution of the noise sources is such that (4) holds true.

The random process $(u(t,\boldsymbol{x}))_{t\in\mathbb{R},\boldsymbol{x}\in\mathbb{R}^3}$ has Gaussian statistics, mean zero, and covariance function (4). An equivalent description of such a random field is:

$$u(t,\boldsymbol{x}) = \int_{\mathbb{R}^3} a(\boldsymbol{k})\exp\big[i(\boldsymbol{k}\cdot\boldsymbol{x}-\Omega(\boldsymbol{k})t)\big]d\boldsymbol{k}, \tag{5}$$

where $\Omega(\boldsymbol{k}) = c_o|\boldsymbol{k}|$ is the dispersion relation of the three-dimensional wave equation and $(a(\boldsymbol{k}))_{\boldsymbol{k}\in\mathbb{R}^3}$ is a complex-valued Gaussian process with mean zero and covariance function

$$\Big\langle a(\boldsymbol{k})\overline{a(\boldsymbol{k}')}\Big\rangle = \mathcal{A}(|\boldsymbol{k}|)\delta(\boldsymbol{k}-\boldsymbol{k}'), \tag{6}$$

with $a(-\boldsymbol{k}) = \overline{a(\boldsymbol{k})}$ and

$$\mathcal{A}(k) = \frac{c_o}{32\pi^3k^2}\hat{F}(c_ok). \tag{7}$$

The proof of the equivalence is straightforward: the random process defined by (5) has Gaussian statistics (as it is a linear transform of a Gaussian process), mean zero, and its covariance is

$$\begin{aligned}\langle u(t,\boldsymbol{x})u(t',\boldsymbol{x}')\rangle &= \int_{\mathbb{R}^3}\exp\big[i\big(\boldsymbol{k}\cdot(\boldsymbol{x}-\boldsymbol{x}')-\Omega(\boldsymbol{k})(t-t')\big)\big]\mathcal{A}(|\boldsymbol{k}|)d\boldsymbol{k} \\ &= \int_0^\infty\int_{\mathbb{S}^3}\exp\big[i\big(k\hat{\boldsymbol{k}}\cdot(\boldsymbol{x}-\boldsymbol{x}')\big]d\hat{\boldsymbol{k}}\,\mathcal{A}(k)\exp\big[-ic_ok(t-t')\big]k^2dk \\ &= 4\pi\int_0^\infty \mathrm{sinc}(k|\boldsymbol{x}-\boldsymbol{x}'|)k^2\mathcal{A}(k)\exp\big[-ic_ok(t-t')\big]dk,\end{aligned}$$

that is equal to (4) after the change of variable $k = \omega/c_o$. This shows that $u(t,\boldsymbol{x})$ can be considered a superposition of uncorrelated plane waves. We are in a situation similar to the one addressed in [3] and we will recover the results of this paper when the medium is homogeneous. However, our approach makes it possible to address non-homogeneous media as we will see in Section 3.

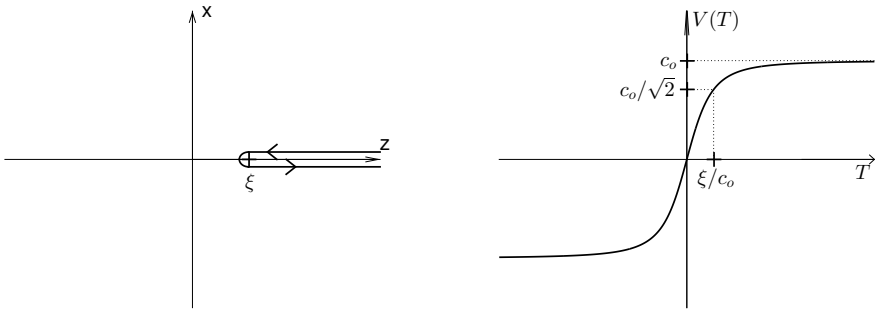

Figure 1: Rindler trajectory (8) in a three-dimensional open medium (left) and speed (along the z-axis) of the Rindler observer in the laboratory frame (right).

2.2. The Wigner transform of the recorded signal

We consider an observer with a Rindler trajectory (see Figure 1, left) whose time-space coordinates are (with fixed $\xi > 0$):

$$T(\tau) = (\xi/c_o)\sinh(c_o\tau/\xi), \qquad \boldsymbol{X}(\tau) = \big(0, 0, \xi\cosh(c_o\tau/\xi)\big), \tag{8}$$

where τ is the proper time (the time as perceived by the accelerated observer). The Rindler trajectory (8) describes a trajectory with constant acceleration [19, 17], in the sense that the acceleration of the observer relative to its instantaneous inertial rest frame is constant and equal to $g = c_o^2/\xi$. In the laboratory frame the trajectory is along the z-axis with the coordinate $Z(T) = \sqrt{\xi^2 + c_o^2T^2}$ and the speed $V(T) = \partial_T Z(T) = c_o^2T/\sqrt{\xi^2 + c_o^2T^2}$ (see Figure 1, right). We will see in the next subsection that this trajectory satisfies a unique property from the point of view of correlation of noise.

The signal recorded by the Rindler observer is

$$U(\tau) = u\big(T(\tau), \boldsymbol{X}(\tau)\big). \tag{9}$$

We look for the properties of the autocorrelation function of the recorded signal:

$$\left\langle U(\tau + \frac{\tau'}{2})U(\tau - \frac{\tau'}{2}) \right\rangle, \tag{10}$$

and the Wigner transform of the recorded signal, that is, its local spectrum:

$$W(\tau, \omega) = \int_{\mathbb{R}} \left\langle U(\tau + \frac{\tau'}{2})U(\tau - \frac{\tau'}{2}) \right\rangle \exp(i\omega\tau')d\tau'. \tag{11}$$

From (4) the autocorrelation function of the noise recorded by the Rindler observer is

$$\begin{aligned}
&\Big\langle U(\tau+\frac{\tau'}{2})U(\tau-\frac{\tau'}{2})\Big\rangle \\
&= \frac{1}{2\pi}\int_{\mathbb{R}} \frac{c_o}{\omega}\hat{F}(\omega)\mathrm{Im}\hat{G}\Big(\omega, \boldsymbol{X}(\tau+\frac{\tau'}{2}), \boldsymbol{X}(\tau-\frac{\tau'}{2})\Big)\exp\Big[i\omega\big(T(\tau+\frac{\tau'}{2})-T(\tau-\frac{\tau'}{2})\big)\Big]d\omega \\
&= \frac{1}{8\pi^2}\int_{\mathbb{R}} \hat{F}(\omega)\mathrm{sinc}\Big(\frac{\omega}{c_o}\big|\boldsymbol{X}(\tau+\frac{\tau'}{2})-\boldsymbol{X}(\tau-\frac{\tau'}{2})\big|\Big)\exp\Big[i\omega\big(T(\tau+\frac{\tau'}{2})-T(\tau-\frac{\tau'}{2})\big)\Big]d\omega.
\end{aligned} \tag{12}$$

We will focus our attention to the case where the source spectrum is of the form

$$\hat{F}(\omega) = f_o|\omega|. \tag{13}$$

We explain in the next subsection the special properties of this source spectrum. Note that, in practice, the source spectrum can be a finite-energy approximation of the ideal spectrum (13), such as $\hat{F}(\omega) = f_o|\omega|\exp(-\epsilon|\omega|)$ for some $\epsilon > 0$ for instance. The following results are then valid in the sense explained in Remark 1.

If the source spectrum is (13) then the power spectral density of the signal recorded by a stationary observer is $f_o|\omega|/(4\pi)$ by (4) (with $\boldsymbol{x}' = \boldsymbol{x}$). For an observer with a Rindler trajectory, we find from (12) that, for any $\tau' \neq 0$ (see Appendix B.1):

$$\Big\langle U(\tau+\frac{\tau'}{2})U(\tau-\frac{\tau'}{2})\Big\rangle = -\frac{c_o^2 f_o}{16\pi^2\xi^2}\frac{1}{\sinh^2(c_o\tau'/(2\xi))}, \tag{14}$$

so that the Wigner transform is independent of τ (see Appendix B.2):

$$W(\tau,\omega) = \frac{f_o}{4\pi}\frac{\omega}{\tanh(\pi\xi\omega/c_o)}. \tag{15}$$

At any time τ, the observer feels the same spectrum. Moreover, the spectrum is a perturbation of the spectrum $f_o|\omega|/(4\pi)$ observed by a stationary observer and it has the "Planck" form:

$$W(\tau,\omega) = W_o(\omega), \qquad W_o(\omega) = \frac{f_o|\omega|}{4\pi}\Big(1+\frac{2}{e^{2\pi\xi|\omega|/c_o}-1}\Big). \tag{16}$$

The analogy with the Planck spectrum is obtained by identifying $2\pi\xi/c_o$ and $\bar{h}/(K_B T)$ (with $\bar{h}$ the Planck's constant divided by 2π, K_B the Boltzmann's constant, and T the Unruh temperature [24]). The result (16) was obtained from the representation (5) in [3, 4]. This representation was convenient to analyze the system in an open medium, but the presence of an obstacle imposes the formulation with noise sources.

Remark 1. *In practice the spectrum may not be equal to (13) but of the form $\hat{F}(\omega) = f_o|\omega|\exp(-\epsilon|\omega|)$ for some $\epsilon > 0$ for instance. This situation is analyzed in Appendix B.3. The autocorrelation function of the recorded signal is then given by (B.4) for any $\epsilon > 0$ which reduces to (14) when ϵ is small and $|\tau'|$ is larger than $O(\epsilon)$. The Wigner transform of the*

recorded signal is given by (B.5) for any $\epsilon > 0$ which reduces to (15) when ϵ is small and ω is smaller than $O(\epsilon^{-1})$. This remark shows that our results are somewhat robust with respect to the form of the source spectrum and that it is possible to consider a source spectrum with finite energy and amplitude while preserving the main results.

Remark 2. *In order to compute the Wigner transform (11) it is necessary to integrate over $\mathbb{R}$. If the signal is only recorded over a finite time interval, then one can compute*

$$W_\chi(\tau,\omega) = \int_{\mathbb{R}} \chi(\tau') \left\langle U(\tau + \frac{\tau'}{2}) U(\tau - \frac{\tau'}{2}) \right\rangle \exp(i\omega\tau') d\tau',$$

where χ is a cut-off function. We then have

$$W_\chi(\tau,\omega) = \int W(\tau, \omega - \omega') \hat{\chi}(\omega') d\omega',$$

where $\hat{\chi}$ is the Fourier transform of χ. If the recording time interval has duration T_c, then this means that we can extract the Wigner transform up to a convolution in ω with a kernel of width $1/T_c$. This remark shows that our results are somewhat robust with respect to the duration of the recording time interval and that it is possible to consider a finite recording time interval while preserving the main results.

2.3. Properties of the source and signal spectra

We recall that we assume that the spatial distribution of the noise sources is such that (4) holds true. The following proposition justifies why we focus our attention to the case where the source spectrum has the form (13).

Proposition 1. *The source spectrum $\hat{F}(\omega) = |\omega|$ (up to a multiplicative constant) is the only Lorentz-invariant spectrum.*

This was proved in [3]. If the source spectrum is Lorentz-invariant, then the signal recorded by an observer with constant velocity has the same spectrum, whatever the velocity of the observer (provided it is constant). This result can be recovered by using our formulation of the problem, except that two possible forms of source spectrum are possible, as stated in the following proposition proved in Appendix B.4.

Proposition 2. *The only source spectra for which the signal recorded by an observer with constant velocity has a spectrum independent of velocity are of the form $\hat{F}(\omega) = f_o|\omega| + f_1/|\omega|$.*

The following proposition proved in Appendix B.5 underlines an important property of a source spectrum of the form (13).

Proposition 3. *The source spectrum $\hat{F}(\omega) = |\omega|$ (up to a multiplicative constant) is the only one for which the recorded signal is stationary (i.e., its autocorrelation function does not depend on τ, or equivalently its Wigner transform does not depend on τ) for a Rindler trajectory.*

The following proposition clarifies a unique and crucial property of the Rindler trajectory.

Proposition 4. *The Rindler trajectories are the only straight-line trajectories for which the recorded signal is stationary (i.e., its autocorrelation function does not depend on τ, or equivalently its Wigner transform does not depend on τ) when the power spectral density of the noise sources is Lorentz invariant (i.e. $\hat{F}(\omega) = f_o|\omega|$).*

Proof. Let us consider a trajectory with proper time τ of the form $(t(\tau), \boldsymbol{x}(\tau))$ with $\boldsymbol{x}(\tau) = (0, 0, z(\tau))$. The time in the laboratory frame t is related to the proper time τ by (B.6). By (4) the autocorrelation function of the recorded signal has the form

$$\begin{aligned}
&\left\langle U(\tau + \frac{\tau'}{2})U(\tau - \frac{\tau'}{2}) \right\rangle \\
&= \frac{f_o}{4\pi^2} \int_0^\infty \frac{\sin\left(\frac{\omega}{c_o}\left|z(\tau + \frac{\tau'}{2}) - z(\tau - \frac{\tau'}{2})\right|\right)}{\frac{1}{c_o}\left|z(\tau + \frac{\tau'}{2}) - z(\tau - \frac{\tau'}{2})\right|} \cos\left(\omega\big(t(\tau + \frac{\tau'}{2}) - t(\tau - \frac{\tau'}{2})\big)\right) d\omega \\
&= \frac{f_o}{4\pi^2} \frac{1}{\frac{1}{c_o^2}\big(z(\tau + \frac{\tau'}{2}) - z(\tau - \frac{\tau'}{2})\big)^2 - \big(t(\tau + \frac{\tau'}{2}) - t(\tau - \frac{\tau'}{2})\big)^2}.
\end{aligned} \tag{17}$$

On the one hand, if the trajectory is Rindler, then there exist t_0, z_0, τ_0, ξ such that $t(\tau) = t_0 + (\xi/c_o)\sinh(c_o(\tau - \tau_0)/\xi)$ and $z(\tau) = z_0 + \xi\cosh(c_o(\tau - \tau_0)/\xi)\big)$, so that

$$\begin{aligned}
t(\tau + \frac{\tau'}{2}) - t(\tau - \frac{\tau'}{2}) =& 2(\xi/c_o)\cosh(c_o(\tau - \tau_0)/\xi)\sinh(c_o\tau'/(2c_o)), \\
z(\tau + \frac{\tau'}{2}) - z(\tau - \frac{\tau'}{2}) =& 2\xi\sinh(c_o(\tau - \tau_0)/\xi)\sinh(c_o\tau'/(2c_o)),
\end{aligned}$$

and therefore

$$\frac{1}{c_o^2}\big(z(\tau + \frac{\tau'}{2}) - z(\tau - \frac{\tau'}{2})\big)^2 - \big(t(\tau + \frac{\tau'}{2}) - t(\tau - \frac{\tau'}{2})\big)^2 = -\frac{4\xi^2}{c_o^2}\sinh^2(c_o\tau'/(2c_o)),$$

which indeed implies that the autocorrelation function of the recorded signal is independent of τ.

On the other hand, if we impose that the autocorrelation function of the recorded signal is independent of τ, then this means that

$$\big(z(\tau + \tau') - z(\tau)\big)^2 - \Big(\int_\tau^{\tau+\tau'} \sqrt{c_o^2 + |\dot{z}(\tau'')|^2}\, d\tau''\Big)^2$$

should be independent of τ, where we have used (B.6). We can expand this expression for small τ' and we get that the fourth-order coefficient of the Taylor series expansion is equal to

$$-\frac{1}{12}\frac{c_o^2\ddot{z}^2}{c_o^2 + \dot{z}^2}.$$

This coefficient should be independent of τ, which means that the function $V = \dot{z}/c_o$ should satisfy an ordinary differential equation of the form

$$\frac{\dot{V}}{\sqrt{1+V^2}} = c_1,$$

for some constant c_1. The general solution of this equation is

$$V(\tau) = \sinh(c_1\tau + c_2),$$

which corresponds to $z(\tau) = c_o/c_1 \cosh(c_1\tau+c_2)+c_3$ and $t(\tau) = (1/c_1)\sinh(c_1\tau+c_2)+c_4$, sor some constants $c_1, \ldots, c_4$. We conclude that the trajectory should be a Rindler trajectory. □

Finally the following proposition shows that the straight-line trajectory hypothesis in Proposition 4 is important.

Proposition 5. *There exist trajectories that do not follow a straight line but that give stationary recorded signals when the power spectral density of the noise sources is of the form* $\hat{F}(\omega) = f_o|\omega|$.

Proof. Let us consider a uniform circular motion with proper time τ of the form $(t(\tau), \boldsymbol{x}(\tau))$ with $\boldsymbol{x}(\tau) = (x(\tau), y(\tau), 0)$,

$$t = \gamma\tau, \quad x(\tau) = \frac{c_o\sqrt{\gamma^2-1}}{p}\cos(p\tau), \quad y(\tau) = \frac{c_o\sqrt{\gamma^2-1}}{p}\sin(p\tau).$$

Here $\gamma > 1$ is the Lorentz factor, $p = \gamma p_0$, p_0 is the coordinate angular velocity. The time in the laboratory frame t is related to the proper time τ by $\dot{t}^2 - (\dot{x}^2+\dot{y}^2)/c_o^2 = 1$. Then we find that

$$\left\langle U(\tau+\frac{\tau'}{2})U(\tau-\frac{\tau'}{2})\right\rangle = \frac{f_o}{4\pi^2}\frac{1}{4\frac{\gamma^2-1}{p^2}\sin^2\left(\frac{p\tau'}{2}\right)-\gamma^2\tau'^2}, \tag{18}$$

which does not depend on τ. The spectrum $W(\tau,\omega)$ is independent of τ as well, it is a perturbation of the spectrum observed by a stationary observer:

$$W(\tau,\omega) = \frac{f_o|\omega|}{4\pi} + \frac{f_o p}{4\pi}W_\gamma(\frac{\omega}{p}),$$

with

$$W_\gamma(w) = \frac{\gamma^2-1}{4\pi^2}\int_{\mathbb{R}}\frac{s^2-\sin^2(s)}{s^2(\gamma^2s^2-(\gamma^2-1)\sin^2(s))}\cos(2ws)ds,$$

which is an even, bounded, and integrable function. The perturbation does not have a Planck form. For $0 \leq \gamma^2-1 \ll 1$, we have

$$\begin{aligned} W_\gamma(w) &= \frac{\gamma^2-1}{4\pi^2}\int_{\mathbb{R}}\frac{s^2-\sin^2(s)}{s^4}\cos(2ws)ds + o(\gamma^2-1) \\ &= \frac{\gamma^2-1}{6\pi}(1-|w|)_+^3 + o(\gamma^2-1). \end{aligned}$$

□

It would be interesting to identify all trajectories that give stationary recorded signals, but this is beyond the scope of this paper. We may conjecture that the result should be that the acceleration should be constant, as it is for the Rindler trajectory and the circular trajectory, but it is not so straightforward. Indeed, if the trajectory $\boldsymbol{x}(\tau) = (x(\tau), y(\tau), z(\tau))$ gives a stationary recorded signal, then the autocorrelation function of the recorded signal

$$\left\langle U(\tau + \frac{\tau'}{2})U(\tau - \frac{\tau'}{2}) \right\rangle = \frac{f_o}{4\pi^2} \frac{1}{\frac{1}{c_o^2}\left|\boldsymbol{x}(\tau + \frac{\tau'}{2}) - \boldsymbol{x}(\tau - \frac{\tau'}{2})\right|^2 - \left(t(\tau + \frac{\tau'}{2}) - t(\tau - \frac{\tau'}{2})\right)^2}$$

should be independent of τ, in other words,

$$\left|\boldsymbol{x}(\tau + \tau') - \boldsymbol{x}(\tau)\right|^2 - \Big(\int_\tau^{\tau+\tau'} \sqrt{c_o^2 + |\dot{\boldsymbol{x}}(\tau'')|^2} d\tau'' \Big)^2$$

should be independent of τ. By following the same strategy as in the proof of Proposition 4, we find that the normalized velocity $\boldsymbol{V} = \dot{\boldsymbol{x}}/c_o$ should satisfy a nonlinear ordinary differential equation of the form

$$|\dot{\boldsymbol{V}}|^2 - \frac{(\boldsymbol{V} \cdot \dot{\boldsymbol{V}})^2}{1 + |\boldsymbol{V}|^2} = c_1,$$

for some constant c_1. However, it does not seem straightforward to identify all the solutions of this equation. Rindler trajectories and uniform circular motions are solutions, but there are other solutions, such as constant helicoidal motions:

$$(x(\tau), y(\tau)) = \frac{c_o\sqrt{\gamma^2 - 1}\sqrt{\alpha}}{p}\big(\cos(p\tau), \sin(p\tau)\big), \quad z(\tau) = c_o\sqrt{\gamma^2 - 1}\sqrt{1 - \alpha}\tau,$$

and $t(\tau) = \gamma\tau$, where τ is the proper time and $\gamma > 1$, $p > 0$, $\alpha \in [0, 1]$ are constant parameters, or uniformly accelerated helicoidal motions:

$$(x(\tau), y(\tau)) = \frac{c_o A}{p}\big(\cos(p\tau), \sin(p\tau)\big), \quad z(\tau) = \xi\sqrt{A^2 + 1}\cosh(c_o\tau/\xi),$$

and $t(\tau) = \sqrt{A^2 + 1}(\xi/c_o)\sinh(c_o\tau/\xi)$, where τ is the proper time and A, ξ, p are constant parameters (we say that this motion is uniformly accelerated because the acceleration along the z-axis of the observer relative to its instantaneous inertial rest frame is constant and equal to $(1 + A^2)c_o^2/\xi$, but the acceleration in the x- and y-directions are not constant). These trajectories also satisfy the property that the signal recorded by a moving observer is stationary.

3. A Rindler observer in front of an obstacle

3.1. The configuration

We consider the three-dimensional scalar wave equation for the scalar wave field $u(t, \boldsymbol{x})$ in the half-space $\mathbb{R}^2 \times (0, +\infty)$:

$$\frac{1}{c_o^2}\partial_t^2 u - \Delta u = n(t, \boldsymbol{x}), \tag{19}$$

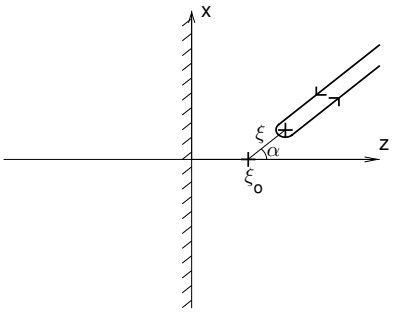

Figure 2: Rindler trajectory (22) with an obstacle in the plane $z = 0$.

with a reflecting (Dirichlet) boundary condition on the plane $z = 0$ (with $\boldsymbol{x} = (x, y, z)$):

$$u(t, (x, y, 0)) = 0. \tag{20}$$

The goal of this section is to show that an observer following a Rindler trajectory can detect and localize the obstacle (i.e. the interface $z = 0$) from the signal that it records.

The source term $n(t, \boldsymbol{x})$ models a noise source distribution. It is a zero-mean process, stationary in time and delta-correlated in space:

$$\langle n(t, \boldsymbol{x}) n(t', \boldsymbol{x}') \rangle = F(t - t') \delta(\boldsymbol{x} - \boldsymbol{x}') K(\boldsymbol{x}), \tag{21}$$

where $K(\boldsymbol{x})$ is the function that characterizes the spatial support of the noise source distribution (it is supported in the half-space $\mathbb{R}^2 \times (0, +\infty)$) and the Fourier transform $\hat{F}(\omega)$ of F is the power spectral density of the sources. For simplicity (this can be easily generalized) we can consider that the function K is spatially supported on a surface of a half-ball $\partial B_+(\mathbf{0}, L) = \{\boldsymbol{x} = (x, y, z) \in \mathbb{R}^3\,,\ z > 0,\ |\boldsymbol{x}| = L\}$ with a very large radius L:

$$K(\boldsymbol{x}) = \delta_{\partial B_+(\mathbf{0}, L)}(\boldsymbol{x}).$$

We consider an observer with a Rindler trajectory whose time-space coordinates are (with fixed $\xi > 0$, $\alpha \in (-\pi/2, \pi/2)$, $\xi_o > -\xi \cos\alpha$):

$$T(\tau) = (\xi/c_o) \sinh(c_o \tau/\xi), \qquad \boldsymbol{X}(\tau) = (0, 0, \xi_o) + \xi \cosh(c_o \tau/\xi) \big(\sin\alpha, 0, \cos\alpha \big), \tag{22}$$

where τ is the proper time of the observer. With this parameterization, the position of the observer is the closest to the obstacle at $\tau = 0$, when it is located at $\boldsymbol{X}(0) = (\xi \sin\alpha, 0, \xi_o + \xi \cos\alpha)$ (see Figure 2). We will first address the direct problem: calculation of the autocorrelation function of the field recorded by the observer. In the inverse problem, the observer knows its acceleration c_o^2/ξ and its proper time τ, it can observe the autocorrelation function of the recorded field and it looks for its relative position to the obstacle, that is to say, it looks for α and ξ_o.

3.2. The Wigner transform of the recorded signal

We first derive an expression of the autocorrelation function in the presence of the obstacle (the interface $z = 0$).

Proposition 6. *The autocorrelation function of the recorded signal has the form*

$$\begin{aligned}
&\Big\langle U(\tau+\frac{\tau'}{2})U(\tau-\frac{\tau'}{2})\Big\rangle \\
&= \frac{1}{8\pi^2}\int_{\mathbb{R}} \hat{F}(\omega)\mathrm{sinc}\Big(\frac{\omega}{c_o}\big|\boldsymbol{X}(\tau+\frac{\tau'}{2})-\boldsymbol{X}(\tau-\frac{\tau'}{2})\big|\Big)\exp\Big[i\omega\big(T(\tau+\frac{\tau'}{2})-T(\tau-\frac{\tau'}{2})\big)\Big]d\omega \\
&\quad - \frac{1}{8\pi^2}\int_{\mathbb{R}} \hat{F}(\omega)\mathrm{sinc}\Big(\frac{\omega}{c_o}\big|\boldsymbol{X}^{\mathrm{s}}(\tau+\frac{\tau'}{2})-\boldsymbol{X}(\tau-\frac{\tau'}{2})\big|\Big)\exp\Big[i\omega\big(T(\tau+\frac{\tau'}{2})-T(\tau-\frac{\tau'}{2})\big)\Big]d\omega,
\end{aligned} \tag{23}$$

with $\boldsymbol{X}^{\mathrm{s}}(\tau) = (0,0,-\xi_o) + \xi\cosh(c_o\tau/\xi)\big(0,\sin\alpha,-\cos\alpha\big)$.

Proof. The expression of the autocorrelation function is

$$\begin{aligned}
\Big\langle U(\tau+\frac{\tau'}{2})U(\tau-\frac{\tau'}{2})\Big\rangle =& \frac{1}{2\pi}\int_{\mathbb{R}}\int_{\mathbb{R}^3} \overline{\hat{\mathcal{G}}\Big(\omega,\boldsymbol{X}(\tau+\frac{\tau'}{2}),\boldsymbol{y}\Big)}\hat{\mathcal{G}}\Big(\omega,\boldsymbol{X}(\tau-\frac{\tau'}{2}),\boldsymbol{y}\Big) \\
&\times K(\boldsymbol{y})\hat{F}(\omega)\exp\Big[i\omega\big(T(\tau+\frac{\tau'}{2})-T(\tau-\frac{\tau'}{2})\big)\Big]d\boldsymbol{y}d\omega.
\end{aligned}$$

Here $\hat{\mathcal{G}}(\omega,\boldsymbol{x},\boldsymbol{y})$ is the Green's function in the presence of the reflecting plane, that is to say

$$\hat{\mathcal{G}}(\omega,\boldsymbol{x},\boldsymbol{y}) = \hat{G}(\omega,\boldsymbol{x},\boldsymbol{y}) - \hat{G}(\omega,\boldsymbol{x},\boldsymbol{y}^{\mathrm{s}}),$$

where $\boldsymbol{y}^{\mathrm{s}} = (y_1,y_2,-y_3)$ is the symmetric point of $\boldsymbol{y} = (y_1,y_2,y_3)$ and $\hat{G}(\omega,\boldsymbol{x},\boldsymbol{y})$ is the three-dimensional homogeneous Green's function (3). Using the fact that $\hat{G}(\omega,\boldsymbol{x},\boldsymbol{y}^{\mathrm{s}}) = \hat{G}(\omega,\boldsymbol{x}^{\mathrm{s}},\boldsymbol{y})$, we find that

$$\begin{aligned}
\Big\langle U(\tau+\frac{\tau'}{2})U(\tau-\frac{\tau'}{2})\Big\rangle =& \frac{1}{2\pi}\int_{\mathbb{R}}\int_{\mathbb{R}^3} \overline{\hat{G}\Big(\omega,\boldsymbol{X}(\tau+\frac{\tau'}{2}),\boldsymbol{y}\Big)}\hat{G}\Big(\omega,\boldsymbol{X}(\tau-\frac{\tau'}{2}),\boldsymbol{y}\Big) \\
&\times \hat{F}(\omega)K^{\mathrm{s}}(\boldsymbol{y})\exp\Big[i\omega\big(T(\tau+\frac{\tau'}{2})-T(\tau-\frac{\tau'}{2})\big)\Big]d\boldsymbol{y}d\omega \\
&- \frac{1}{2\pi}\int_{\mathbb{R}}\int_{\mathbb{R}^3} \overline{\hat{G}\Big(\omega,\boldsymbol{X}^{\mathrm{s}}(\tau+\frac{\tau'}{2}),\boldsymbol{y}\Big)}\hat{G}\Big(\omega,\boldsymbol{X}(\tau-\frac{\tau'}{2}),\boldsymbol{y}\Big) \\
&\times \hat{F}(\omega)K^{\mathrm{s}}(\boldsymbol{y})\exp\Big[i\omega\big(T(\tau+\frac{\tau'}{2})-T(\tau-\frac{\tau'}{2})\big)\Big]d\boldsymbol{y}d\omega,
\end{aligned}$$

where we have defined

$$K^{\mathrm{s}}(\boldsymbol{y}) = K(\boldsymbol{y}) + K(\boldsymbol{y}^{\mathrm{s}}).$$

As we assume that $K(\boldsymbol{x}) = \delta_{\partial B_+(\mathbf{0},L)}(\boldsymbol{x})$, K^{s} is supported at the surface of the ball with center at $\mathbf{0}$ and radius L, i.e. $K^{\mathrm{s}}(\boldsymbol{x}) = \delta_{\partial B(\mathbf{0},L)}(\boldsymbol{x})$, so we can invoke Helmholtz-Kirchhoff identity (A.1) to compute the integral in $\boldsymbol{y}$ and we get

$$\begin{aligned}
&\Big\langle U(\tau+\frac{\tau'}{2})U(\tau-\frac{\tau'}{2})\Big\rangle \\
&= \frac{1}{2\pi}\int_{\mathbb{R}} \frac{c_o}{\omega}\hat{F}(\omega)\mathrm{Im}\hat{G}\Big(\omega, \boldsymbol{X}(\tau+\frac{\tau'}{2}), \boldsymbol{X}(\tau-\frac{\tau'}{2})\Big)\exp\Big[i\omega\big(T(\tau+\frac{\tau'}{2})-T(\tau-\frac{\tau'}{2})\big)\Big]d\omega \\
&\quad - \frac{1}{2\pi}\int_{\mathbb{R}} \frac{c_o}{\omega}\hat{F}(\omega)\mathrm{Im}\hat{G}\Big(\omega, \boldsymbol{X}^{\mathrm{s}}(\tau+\frac{\tau'}{2}), \boldsymbol{X}(\tau-\frac{\tau'}{2})\Big)\exp\Big[i\omega\big(T(\tau+\frac{\tau'}{2})-T(\tau-\frac{\tau'}{2})\big)\Big]d\omega.
\end{aligned} \tag{24}$$

We can rewrite this equation in two explicit forms, either (23) or

$$\begin{aligned}
&\Big\langle U(\tau+\frac{\tau'}{2})U(\tau-\frac{\tau'}{2})\Big\rangle \\
&= \frac{1}{8\pi}\int_{-1}^{1} F\Big(\frac{v}{c_o}\big|\boldsymbol{X}(\tau+\frac{\tau'}{2})-\boldsymbol{X}(\tau-\frac{\tau'}{2})\big| + \big(T(\tau+\frac{\tau'}{2})-T(\tau-\frac{\tau'}{2})\big)\Big)dv \\
&\quad - \frac{1}{8\pi}\int_{-1}^{1} F\Big(\frac{v}{c_o}\big|\boldsymbol{X}^{\mathrm{s}}(\tau+\frac{\tau'}{2})-\boldsymbol{X}(\tau-\frac{\tau'}{2})\big| + \big(T(\tau+\frac{\tau'}{2})-T(\tau-\frac{\tau'}{2})\big)\Big)dv.
\end{aligned} \tag{25}$$

The form (25) is obtained by using the explicit form (3) of the Green's function and the identity $\int_{-1}^{1}\exp(ivs)dv = 2\mathrm{sinc}(s)$, so that

$$\begin{aligned}
&\int_{\mathbb{R}} \frac{c_o}{\omega}\hat{F}(\omega)\mathrm{Im}\hat{G}\Big(\omega, \boldsymbol{X}(\tau+\frac{\tau'}{2}), \boldsymbol{X}(\tau-\frac{\tau'}{2})\Big)\exp\Big[i\omega\big(T(\tau+\frac{\tau'}{2})-T(\tau-\frac{\tau'}{2})\big)\Big]d\omega \\
&= \frac{1}{4\pi}\int_{\mathbb{R}} \hat{F}(\omega)\mathrm{sinc}\Big(\frac{\omega}{c_o}\big|\boldsymbol{X}(\tau+\frac{\tau'}{2})-\boldsymbol{X}(\tau-\frac{\tau'}{2})\big|\Big)\exp\Big[i\omega\big(T(\tau+\frac{\tau'}{2})-T(\tau-\frac{\tau'}{2})\big)\Big]d\omega \\
&= \frac{1}{8\pi}\int_{-1}^{1} dv\int_{\mathbb{R}} \hat{F}(\omega)\exp\Big[i\frac{\omega v}{c_o}\big|\boldsymbol{X}(\tau+\frac{\tau'}{2})-\boldsymbol{X}(\tau-\frac{\tau'}{2})\big|\Big]\exp\Big[i\omega\big(T(\tau+\frac{\tau'}{2})-T(\tau-\frac{\tau'}{2})\big)\Big]d\omega \\
&= \frac{1}{4}\int_{-1}^{1} dv F\Big(\frac{v}{c_o}\big|\boldsymbol{X}(\tau+\frac{\tau'}{2})-\boldsymbol{X}(\tau-\frac{\tau'}{2})\big| + \big(T(\tau+\frac{\tau'}{2})-T(\tau-\frac{\tau'}{2})\big)\Big),
\end{aligned}$$

and similarly for the second term in (24). □

From now on we assume that the power spectral density of the sources is of the form (13). If the observer is stationary at position $\boldsymbol{X}_0$, then we have from (23) taken with $\boldsymbol{X}(\tau)\equiv\boldsymbol{X}_0$ and $T(\tau)\equiv\tau$:

$$\begin{aligned}
\Big\langle u(\tau+\frac{\tau'}{2},\boldsymbol{X}_0)u(\tau-\frac{\tau'}{2},\boldsymbol{X}_0)\Big\rangle &= \frac{1}{8\pi^2}\int_{\mathbb{R}} f_o|\omega|\exp(i\omega\tau')d\omega \\
&\quad - \frac{1}{8\pi^2}\int_{\mathbb{R}} f_o|\omega|\mathrm{sinc}\Big(\frac{\omega}{c_o}\big|\boldsymbol{X}_0^{\mathrm{s}}-\boldsymbol{X}_0\big|\Big)\exp(i\omega\tau')d\omega,
\end{aligned}$$

and therefore

$$\int_{\mathbb{R}} \left\langle u(\tau+\frac{\tau'}{2},\boldsymbol{X}_0)u(\tau-\frac{\tau'}{2},\boldsymbol{X}_0)\right\rangle \exp(i\omega\tau')d\tau' = \frac{f_o|\omega|}{4\pi}\Big(1-\operatorname{sinc}\Big(\frac{\omega}{c_o}|\boldsymbol{X}_0^{\rm s}-\boldsymbol{X}_0|\Big)\Big).$$

This shows that the unperturbed spectrum $f_o|\omega|/(4\pi)$ felt by a stationary observer in a homogeneous medium is perturbed by the obstacle and that the observer can extract the distance $|\boldsymbol{X}_0^{\rm s}-\boldsymbol{X}_0|$ from the spectrum, that is to say, twice the distance from the observer to the obstacle. However, the observer cannot determine the angular position of the obstacle, which is not surprising by symmetry of the system.

Let us now consider an observer on a Rindler trajectory. By (23) we have

$$\begin{aligned}\left\langle U(\tau+\frac{\tau'}{2})U(\tau-\frac{\tau'}{2})\right\rangle = &-\frac{c_o^2 f_o}{16\pi^2\xi^2}\frac{1}{\sinh^2(\eta'/2)}\\ &+\frac{c_o^2 f_o}{16\pi^2\xi^2}\frac{1}{A\cosh^2(\eta'/2)+B(\eta)\cosh(\eta'/2)+C(\eta)},\end{aligned}\tag{26}$$

where $\eta = c_o\tau/\xi$ and $\eta' = c_o\tau'/\xi$,

$$A=\sin^2\alpha,\qquad B(\eta)=-2\alpha_o\cos\alpha\cosh\eta,\qquad C(\eta)=-1-\alpha_o^2-\cos^2\alpha\sinh^2\eta,\tag{27}$$

and $\alpha_o = \xi_o/\xi$. The first term in the right-hand side of (26) gives the constant Planck spectrum that is observed when the observer moves in a homogeneous medium. The second term gives the perturbation of the Planck spectrum that depends on τ and that is induced by the obstacle. The calculation of the Wigner transform requires the following lemma.

Lemma 1. *For $a\in[0,1)$, $b\in\mathbb{R}$, and $c\le -1$, with $a+c+|b|<0$, we define the integral*

$$\Psi(v;a,b,c)=\int_{\mathbb{R}}\frac{\exp(ivs)}{a\cosh^2(s)+b\cosh(s)+c}ds.\tag{28}$$

1. *If $a\in(0,1)$ and $b\neq 0$, then*

$$\Psi(v;a,b,c)=-\frac{2\pi}{\sqrt{\Delta}}\Big\{\frac{\sin\big[v\operatorname{argcosh}(c_+)\big]}{\tanh(\pi v)\sqrt{c_+^2-1}}+\frac{\sin\big[v\operatorname{argcosh}(|c_-|)\big]}{\sinh(\pi v)\sqrt{c_-^2-1}}\Big\},\tag{29}$$

where

$$c_\pm=\frac{-b\pm\sqrt{\Delta}}{2a},\qquad \Delta=b^2-4ac.$$

2. *If $a=0$ and $b\neq 0$, then*

$$\Psi(v;0,b,c)=-\frac{2\pi}{\sqrt{c^2-b^2}\sinh(\pi v)}\sin\big[v\operatorname{argcosh}(\sqrt{c/b})\big].\tag{30}$$

3. *If $a\in(0,1)$ and $b=0$, then*

$$\Psi(v;a,0,c)=-\frac{\pi}{\sqrt{c^2+ca}\tanh(\pi v/2)}\sin\big[v\operatorname{argcosh}(\sqrt{-c/a})\big].\tag{31}$$

4. *If* $a = 0$ *and* $b = 0$, *then*

$$\Psi(v; 0, 0, c) = \frac{2\pi}{c}\delta(v). \tag{32}$$

This lemma can be proved by the residue theorem (see Appendix B.6) and it can be applied to prove the following proposition.

Proposition 7. *The Wigner transform* $W(\tau, \omega)$ *of the recorded signal is a deformed version of the Planck spectrum* $W_o(\omega)$ *defined by (16):*

$$W(\tau, \omega) = W_o(\omega)\big[1 - R(c_o\tau/\xi, \xi\omega/c_o)\big]. \tag{33}$$

The correction R *has the following form:*
- If the observer trajectory is not normally incident, $\alpha \neq 0$, *then*

$$\begin{aligned} R(\eta, \nu) =& \frac{\tanh(\pi\nu)}{\nu \tanh(2\pi\nu)} \frac{\sin\big[2\nu \operatorname{argcosh}(C_+(\eta))\big]}{\sqrt{B^2(\eta) - 4AC(\eta)}\sqrt{C_+^2(\eta) - 1}} \\ &+ \frac{\tanh(\pi\nu)}{\nu \sinh(2\pi\nu)} \frac{\sin\big[2\nu \operatorname{argcosh}(|C_-(\eta)|)\big]}{\sqrt{B^2(\eta) - 4AC(\eta)}\sqrt{C_-^2(\eta) - 1}}, \end{aligned} \tag{34}$$

where

$$C_\pm(\eta) = \frac{-B(\eta) \pm \sqrt{B^2(\eta) - 4AC(\eta)}}{2A},$$

and $A, B(\eta), C(\eta)$ *are given by (27).*
- If the observer trajectory is normally incident, $\alpha = 0$, *then*

$$R(\eta, \nu) = \begin{cases} \dfrac{\tanh(\pi\nu)}{\tanh(2\pi\nu)} \dfrac{\sin\big[2\nu \operatorname{argcosh}(|C(\eta)/B(\eta)|)\big]}{\nu\sqrt{C^2(\eta) - B^2(\eta)}} & \text{if } \alpha_o \in (-1, 0), \\ \dfrac{\tanh(\pi\nu)}{\sinh(2\pi\nu)} \dfrac{\sin\big[\nu \operatorname{argcosh}(|C(\eta)/B(\eta)|)\big]}{2\nu\sqrt{C^2(\eta) - B^2(\eta)}} & \text{if } \alpha_o \in (0, +\infty), \\ 0 & \text{if } \alpha_o = 0, \end{cases} \tag{35}$$

where $B(\eta), C(\eta)$ *are given by (27).*

Eq. (35) can also be written as

$$R(\eta, \nu) = \begin{cases} \Big(1 - \dfrac{1}{2\cosh^2(\pi\nu)}\Big) \dfrac{\sin\big[2\nu \ \ln(\cosh(\eta)/|\alpha_o|)\big]}{\nu\big(\cosh^2(\eta) - \alpha_o^2\big)} & \text{if } \alpha_o \in (-1, 0), \\ \dfrac{1}{2\cosh^2(\pi\nu)} \dfrac{\sin\big[2\nu \ \ln(\alpha_o/\cosh(\eta))\big]}{\nu\big(\alpha_o^2 - \cosh^2(\eta)\big)} & \text{if } \alpha_o \in (0, +\infty), \\ 0 & \text{if } \alpha_o = 0. \end{cases} \tag{36}$$

This proposition shows how the position of the obstacle relative to the observer is encoded in the perturbation of the Wigner transform of the recorded signal.

3.3. The localization of the obstacle

The obstacle can be detected by the observer except in the special situation when $\alpha = 0$ and $\xi_o = 0$. We then have:

$$\left\langle U(\tau + \frac{\tau'}{2})U(\tau - \frac{\tau'}{2}) \right\rangle = -\frac{c_o^2 f_o}{16\pi^2\xi^2}\frac{1}{\sinh^2(\eta'/2)} - \frac{c_o^2 f_o}{16\pi^2\xi^2}\frac{1}{\cosh^2(\eta)},$$

where $\eta = c_o\tau/\xi$ and $\eta' = c_o\tau'/\xi$, so that the perturbation of the Wigner transform is proportional to $\delta(\omega)$, which does not affect the spectrum at any $\omega \neq 0$. This was observed in [21], but we show here that this result only hold true for a very particular situation, when the Rindler trajectory is normally incident ($\alpha = 0$) and stops at exactly the distance ξ from the obstacle ($\xi_0 = 0$).

In general, when $|\eta| \gg 1$, i.e. when the observer is far from the obstacle, then $C_\pm(\eta) \sim \cosh(\eta)$ and $R(\eta, \nu)$ is negligible.

In Figure 3 the correction $R(\eta, \nu)$ is plotted when the trajectory has normal incidence $\alpha = 0$. When the observer comes close to the obstacle (i.e. when ξ_o is close to $-\xi$ and $\eta \simeq 0$) the correction is close to one for a large band of frequencies:

$$R(\eta, \nu) \overset{\xi_o \simeq -\xi,\, \eta \simeq 0}{\simeq} 1 - \frac{1}{2\cosh^2(\pi\nu)},$$

which makes it easy for the observer to detect the correction, hence the obstacle. The fact that the correction is approximately one comes from the Dirichlet boundary condition at the boundary of the obstacle, which makes the field approximately zero close to the boundary. When the observer is far from the obstacle (for large η) the correction is close to zero. When the observer is in the neighborhood of the obstacle, the correction has a complicated frequency-dependent structure. The maximal correction is reached at positive frequency when $\xi_o < 0$ and at zero-frequency when $\xi_o > 0$. The correction can be larger than one. There is no contradiction, the Wigner transform can take (locally in η) negative values.

In Figure 4, the correction $R(\eta, \nu)$ is plotted when the trajectory has normal incidence $\alpha = 0$ and α_o is very close to zero. This illustrates the above remark that the correction is in this case concentrated at very small frequencies, and that in the limit $\alpha_o \to 0$ it is proportional to $\delta(\nu)$.

In Figure 5 the correction $R(\eta, \nu)$ is plotted when the trajectory has oblique incidence $\alpha = \pi/4$. The results are quantitatively different, but qualitatively similar. In particular, when the observer is very close to the obstacle ($\xi_o \simeq -\xi\cos(\alpha)$, $\eta \simeq 0$) then the correction is close to one for a large band of frequencies because of the Dirichlet condition:

$$R(\eta, \nu) \overset{\xi_o \simeq -\xi\cos\alpha,\, \eta \simeq 0}{\simeq} 1 - \frac{1}{2\cosh^2(\pi\nu)}\left(1 - \frac{\sin\left[2\nu\,\mathrm{argcosh}(1 + 2/\tan^2\alpha)\right]}{4\nu\sqrt{1/\tan^2\alpha + 1/\tan^4\alpha}}\right).$$

In the point of view of the inverse problem, one could implement an optimal control strategy to minimize the least square mismatch between an observed spectrum correction and the theoretical spectrum correction parameterized by α and α_o. This can be done for a given time τ, or for several τ in order to improve the resolution and the robustness of the estimation method. These are standard procedures [1].

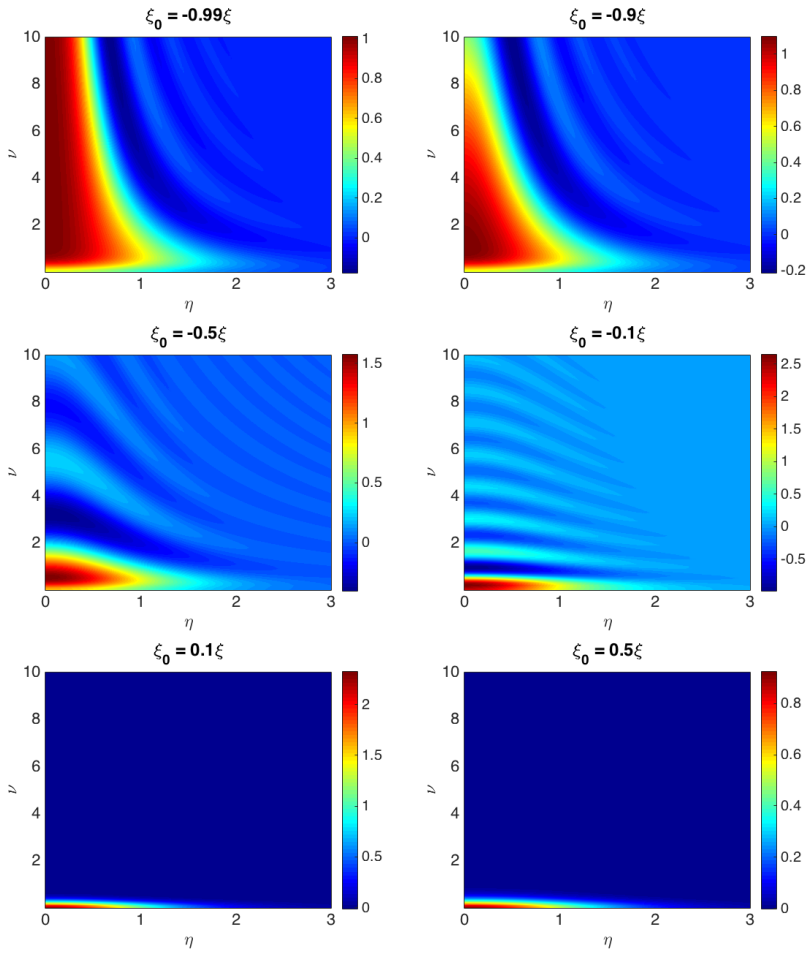

Figure 3: Correction $R(\eta, \nu)$ when $\alpha = 0$ (normal incidence). The correction R is defined in (33), as a function of $\eta = c_o\tau/\xi$ and $\nu = \xi\omega/c_o$. When $\xi_o = -0.99\xi$ and $\eta = 0$, the observer is at distance 0.01ξ from the obstacle (the trajectory is given by (22)).

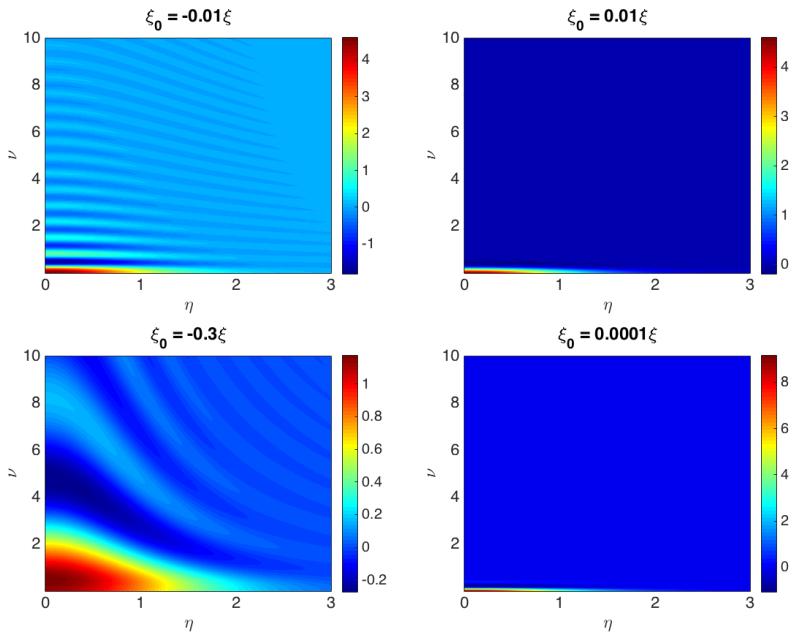

Figure 4: Correction $R(\eta, \nu)$ when $\alpha = 0$ (normal incidence) and $\alpha_o = \xi_o/\xi$ is close to zero. The correction becomes proportional to $\delta(\nu)$.

4. Conclusion

The results reported in this paper show that, as long as a Rindler observer is far from an obstacle, it perceives a constant Planck spectrum when the illumination comes from noise sources with Lorentz-invariant spectrum. However, when the observer comes into the neighborhood of an obstacle, the Wigner transform of the recorded signal deviates from the Planck spectrum and the deviation can be used to localize the obstacle. This demonstrates that a passive observer can perceive its environment from the signal that it records and that is transmitted by noise sources.

In this paper the obstacle has the form of an infinite perfect mirror. It would be interesting to address more general obstacles, for which the curvature of the obstacle surface would be important [9]. This result could also be extended qualitatively to other trajectories: an obstacle would modify the Wigner transform of the recorded signal. However the Rindler trajectory is the unique straight-line trajectory that allows the observer to feel a constant spectrum whatever its time or position, as long as the observer is far from any obstacle. It is only when it comes into the neighborhood of an obstacle that the spectrum is modified, which allows the observer to detect the obstacle and to determine its relative position with respect to the obstacle once the entire trajectory has been traversed. Finally, this paper only addresses noise sources with Lorentz-invariant spectra. If we look for other applications, other spectra may be more appropriate. Remarks 1 and 2 seem to indicate that our main results are somewhat robust with respect to the form of the source spectrum and the duration of the recording time window, but more detailed work is needed to quantify the

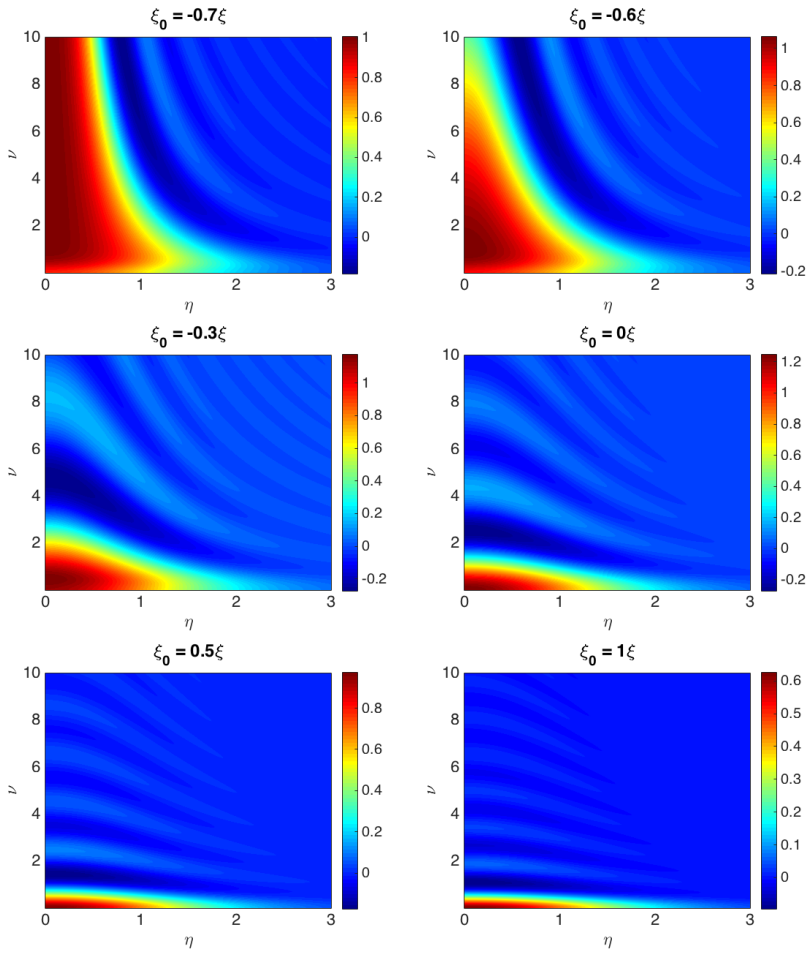

Figure 5: Correction $R(\eta, \nu)$ when $\alpha = \pi/4$ (oblique incidence). When $\xi_o = -0.7\xi$ and $\eta = 0$, the observer is at distance 0.0071ξ from the obstacle.

loss of accuracy and resolution in these general cases.

Acknowledgments

This work was partially supported by LABEX WIFI (Laboratory of Excellence ANR-10-LABX-24) within the French Program Investments for the Future under reference ANR-10-IDEX-0001-02 PSL*.

Appendix A. Helmholtz-Kirchhoff identity

For any $\boldsymbol{x}_1, \boldsymbol{x}_2 \in \mathbb{R}^3$ we have for $L \to \infty$:

$$\mathrm{Im}\hat{G}(\omega, \boldsymbol{x}_1, \boldsymbol{x}_2) = \frac{\omega}{c_o} \int_{\partial B(\mathbf{0},L)} \overline{\hat{G}(\omega, \boldsymbol{x}_1, \boldsymbol{y})} \hat{G}(\omega, \boldsymbol{x}_2, \boldsymbol{y}) d\sigma(\boldsymbol{y}), \tag{A.1}$$

where $d\sigma(\boldsymbol{y})$ is the surface integral. It is a consequence of second Green's identity and Sommerfeld radiation condition [14].

Appendix B. Proofs

Appendix B.1. Proof of (14)

We consider (12) with $\hat{F}(\omega) = |\omega|$ and $\tau' \neq 0$. We denote $\eta = c_o\tau/\xi$ and $\eta' = c_o\tau'/\xi$. By (8), we have

$$\begin{aligned}
\big|\boldsymbol{X}(\tau + \frac{\tau'}{2}) - \boldsymbol{X}(\tau - \frac{\tau'}{2})\big| &= 2\xi \big|\sinh(\eta)\sinh(\frac{\eta'}{2})\big|, \\
T(\tau + \frac{\tau'}{2}) - T(\tau - \frac{\tau'}{2})\big) &= 2\xi \cosh(\eta)\sinh(\frac{\eta'}{2}),
\end{aligned}$$

so that

$$\begin{aligned}
\left\langle U(\tau + \frac{\tau'}{2})U(\tau - \frac{\tau'}{2}) \right\rangle =& \frac{1}{4\pi^2} \frac{1}{\frac{2\xi}{c_o}\sinh(\eta)\sinh(\frac{\eta'}{2})} \\
&\times \int_0^\infty \sin\Big(\frac{\omega}{c_o} 2\xi \sinh(\eta)\sinh(\frac{\eta'}{2})\Big) \cos\Big(\frac{\omega}{c_o} 2\xi \cosh(\eta)\sinh(\frac{\eta'}{2})\Big) d\omega \\
=& \frac{1}{8\pi^2} \frac{1}{\frac{2\xi}{c_o}\sinh(\eta)\sinh(\frac{\eta'}{2})} \int_0^\infty \sin\Big(\frac{\omega}{c_o} 2\xi \sinh(\frac{\eta'}{2})[\sinh(\eta) + \cosh(\eta)]\Big) \\
&+ \sin\Big(\frac{\omega}{c_o} 2\xi \sinh(\frac{\eta'}{2})[\sinh(\eta) - \cosh(\eta)]\Big) d\omega.
\end{aligned}$$

We have (for the justification of the inversion of the integral and the limit $\epsilon \to 0$, see Appendix B.3)

$$\int_0^\infty \sin(\omega t) d\omega = \mathrm{Im} \lim_{\epsilon \to 0^+} \int_0^\infty e^{(it-\epsilon)\omega} d\omega = \mathrm{Im} \frac{-1}{it - \epsilon} = \frac{1}{t}, \tag{B.1}$$

so that

$$\left\langle U(\tau+\frac{\tau'}{2})U(\tau-\frac{\tau'}{2})\right\rangle = \frac{1}{8\pi^2}\frac{1}{\frac{2\xi}{c_o}\sinh(\eta)\sinh(\frac{\eta'}{2})} \times\Big[\frac{1}{\frac{2\xi}{c_o}\sinh(\frac{\eta'}{2})[\sinh(\eta)+\cosh(\eta)]}+\frac{1}{\frac{2\xi}{c_o}\sinh(\frac{\eta'}{2})[\sinh(\eta)-\cosh(\eta)]}\Big] = -\frac{c_o^2}{16\pi^2\xi^2\sinh^2(\frac{\eta'}{2})}.$$

Appendix B.2. Proof of (15)

We show that the inverse Fourier transform of $\omega\mapsto W(\tau,\omega)$ defined by (15) gives (14) for any $\tau'\neq 0$ (the proof follows closely [3]):

$$\frac{1}{2\pi}\int_{\mathbb{R}} W(\tau,\omega)e^{-i\omega\tau'}d\omega = \frac{f_o}{4\pi^2}\int_0^\infty \frac{\omega}{\tanh(\pi\xi\omega/c_o)}\cos(\omega\tau')d\omega = \frac{f_o}{4\pi^2}\Big\{\int_0^\infty \omega\cos(\omega\tau')d\omega+\int_0^\infty\frac{2\omega\cos(\omega\tau')}{\exp(2\pi\xi\omega/c_o)-1}d\omega\Big\}.$$

The singular part can be computed by

$$\int_0^\infty \omega\cos(\omega t)d\omega = \mathrm{Re}\lim_{\epsilon\to 0^+}\int_0^\infty \omega e^{(it-\epsilon)\omega}d\omega = -\frac{1}{t^2}, \tag{B.2}$$

and by using [16, formula 3.951.5] we get the expression of the regular part, so that we obtain

$$\frac{1}{2\pi}\int_{\mathbb{R}} W(\tau,\omega)e^{-i\omega\tau'}d\omega = \frac{f_o}{4\pi^2}\Big\{-\frac{1}{\tau'^2}+\Big[\frac{1}{\tau'^2}-\frac{\frac{c_o^2}{4\xi^2}}{\sinh^2(c_o\tau'/(2\xi))}\Big]\Big\},$$

which gives (15).

Appendix B.3. Finite-energy spectrum

Here we revisit the two previous appendices when the source spectrum is of the form

$$\hat{F}(\omega) = f_o|\omega|\exp(-\epsilon|\omega|) \tag{B.3}$$

for some $\epsilon>0$. The goal is twofold: First we want to justify the inversion of the integral and the limit $\epsilon\to 0$ in (B.1) and (B.2). Second we want to show that we can deal with a noise source spectrum with finite energy and amplitude, and therefore classical recorded signals with finite energy and amplitude, without altering the results.

By (8), we have

$$\left\langle U(\tau+\frac{\tau'}{2})U(\tau-\frac{\tau'}{2})\right\rangle = \frac{1}{8\pi^2}\frac{1}{\frac{2\xi}{c_o}\sinh(\eta)\sinh(\frac{\eta'}{2})}\int_0^\infty\Big[\sin\Big(\frac{\omega}{c_o}2\xi\sinh(\frac{\eta'}{2})e^{\eta}\Big) - \sin\Big(\frac{\omega}{c_o}2\xi\sinh(\frac{\eta'}{2})e^{-\eta}\Big)\Big]\exp(-\epsilon\omega)d\omega.$$

Then, using

$$\int_0^\infty \sin(\omega t)\exp(-\epsilon\omega)d\omega = \mathrm{Im}\int_0^\infty e^{(it-\epsilon)\omega}d\omega = \mathrm{Im}\frac{-1}{it-\epsilon} = \frac{t}{t^2+\epsilon^2},$$

we find that, for any $\epsilon > 0$:

$$\left\langle U(\tau+\frac{\tau'}{2})U(\tau-\frac{\tau'}{2})\right\rangle = \frac{1}{8\pi^2\sinh(\eta)}\Big[\frac{e^{\eta}}{\left(\frac{2\xi}{c_o}\right)^2\sinh(\frac{\eta'}{2})^2e^{2\eta}+\epsilon^2} - \frac{e^{-\eta}}{\left(\frac{2\xi}{c_o}\right)^2\sinh(\frac{\eta'}{2})^2e^{-2\eta}+\epsilon^2}\Big]. \tag{B.4}$$

The limit $\epsilon \to 0$ can be taken in this expression to get that (14) gives the correct value of the autocorrelation function of the recorded signal when the source spectrum is (B.3) and $\sinh(c_o|\tau'|/(2\xi)) > (c_o\epsilon/\xi)\exp(c_o|\tau|/\xi)$, i.e. $|\tau'| > O(\epsilon)$.

A similar analysis can be carried out for the Wigner transform of the recorded signal (11). Using [16, formula 3.983.1], we get that, for any $\epsilon > 0$,

$$\begin{aligned} W(\tau,\omega) =& \frac{c_o}{4\pi\xi(e^{2\eta}-1)}\frac{\sinh\left(\frac{\omega\xi}{c_o}\arccos\left(-1+\frac{c_o^2}{2\xi^2}e^{-2\eta}\epsilon^2\right)\right)}{\sqrt{1-(1-\frac{c_o^2}{2\xi^2}e^{-2\eta}\epsilon^2)^2}\sinh\left(\frac{\omega\xi\pi}{c_o}\right)} \\ &+ \frac{c_o}{4\pi\xi(e^{-2\eta}-1)}\frac{\sinh\left(\frac{\omega\xi}{c_o}\arccos\left(-1+\frac{c_o^2}{2\xi^2}e^{2\eta}\epsilon^2\right)\right)}{\sqrt{1-(1-\frac{c_o^2}{2\xi^2}e^{2\eta}\epsilon^2)^2}\sinh\left(\frac{\omega\xi\pi}{c_o}\right)}. \end{aligned} \tag{B.5}$$

The limit $\epsilon \to 0$ can be taken in this expression (using $\arccos(-1+s) = \pi - \sqrt{2s} + O(s^{3/2})$ and $\sqrt{1-(1-s)^2} = \sqrt{2s} + O(s^{3/2})$ as $s \to 0$) to get that (15) gives the correct value of the Wigner transform of the recorded signal when the source spectrum is (B.3) and $c_o/\xi + |\omega| < \epsilon^{-1}\exp(-c_o|\tau|/\xi)$, i.e. $|\omega| < O(\epsilon^{-1})$.

Appendix B.4. Proof of Proposition 2

A stationary observer records the signal $U(\tau) = u(\tau, \boldsymbol{x}_0)$ whose autocorrelation function is

$$\left\langle U(\tau+\frac{\tau'}{2})U(\tau-\frac{\tau'}{2})\right\rangle = \frac{1}{8\pi^2}\int_{\mathbb{R}}\hat{F}(\omega)\exp(i\omega\tau)d\omega.$$

Let us consider an observer moving along the z-axis at the constant velocity $v > 0$. The trajectory with proper time τ is of the form $(t(\tau), \boldsymbol{x}(\tau))$ with $\boldsymbol{x}(\tau) = (0, 0, z(\tau))$. The time in the laboratory frame t is related to the proper time τ by

$$\dot{t}^2 - \dot{z}^2/c_o^2 = 1, \tag{B.6}$$

with $\dot{t} = \partial_\tau t$, $\dot{z} = \partial_\tau z$ (this comes from the fact that the Minkowski metric is $ds^2 = c_o^2dt^2 - dz^2$ and the proper time τ is s/c_o). Without loss of generality (since the medium is invariant by any spatial shift), we can assume $t(0) = 0$ and $z(0) = 0$. As the velocity v is constant, we have $\frac{dz}{dt} = v$, or $\dot{z} = v\dot{t}$. Substituting into (B.6) this gives $\dot{t} = \gamma$, with $\gamma = 1/\sqrt{1-v^2/c_o^2}$

(Lorentz factor), and therefore $t(\tau) = \gamma\tau$ and $z(\tau) = \gamma v\tau$. From (4) the autocorrelation function of the recorded signal $U(\tau) = u(t(\tau), \boldsymbol{x}(\tau))$ has the form

$$\left\langle U(\tau + \frac{\tau'}{2})U(\tau - \frac{\tau'}{2}) \right\rangle = \frac{1}{8\pi^2} \int_{\mathbb{R}} \hat{F}(\omega) \mathrm{sinc}\Big(\frac{\omega}{c_o}\gamma v\tau'\Big) \exp(i\omega\gamma\tau')d\omega, \tag{B.7}$$

which is a function of τ' only, which may depend on v. We want to identify the source spectrum $\hat{F}$ such that the autocorrelation function (or equivalently the Wigner transform) does not depend on v. Using the fact that, for any $\alpha > 0$,

$$\int_{\mathbb{R}} \mathrm{sinc}(\alpha s) \exp(-i\Omega s)ds = \frac{\pi}{\alpha}\mathbf{1}_{[-\alpha,\alpha]}(\Omega),$$

we find that the Wigner transform is, for $\omega > 0$,

$$W(\tau, \omega) = \frac{1}{8\pi\gamma\frac{v}{c_o}} \int_{\frac{\omega}{\gamma(1+\frac{v}{c_o})}}^{\frac{\omega}{\gamma(1-\frac{v}{c_o})}} \hat{F}_1(\omega')d\omega', \tag{B.8}$$

with $\hat{F}_1(\omega) = \hat{F}(\omega)/\omega$. The Wigner transform can be expanded for small v/c_o as

$$W(\tau, \omega) = \frac{1}{4\pi}\hat{F}_1(\omega) + \frac{v^2}{8\pi c_o^2}\Big[\omega\partial_\omega\hat{F}_1(\omega) + \frac{\omega^2}{3}\partial_\omega^2\hat{F}_1(\omega)\Big] + o\Big(\frac{v^2}{c_o^2}\Big).$$

Therefore, a necessary condition for the Wigner transform to be independent of v is that $\hat{F}_1$ should satisfy $\omega\partial_\omega\hat{F}_1(\omega) + \frac{\omega^2}{3}\partial_\omega^2\hat{F}_1(\omega) = 0$, that is to say, $\hat{F}_1(\omega)$ should be of the form $\hat{F}_1(\omega) = f_o + \frac{f_1}{\omega^2}$, or

$$\hat{F}(\omega) = f_o|\omega| + \frac{f_1}{|\omega|}. \tag{B.9}$$

It turns out that (B.9) is also a sufficient condition. Indeed, if $\hat{F}(\omega) = f_o|\omega|$, then (B.8) gives (for $\omega > 0$)

$$W(\tau, \omega) = \frac{f_o}{8\pi\gamma\frac{v}{c_o}}\Big(\frac{\omega}{\gamma(1-\frac{v}{c_o})} - \frac{\omega}{\gamma(1+\frac{v}{c_o})}\Big) = \frac{f_o\omega}{4\pi},$$

and if $\hat{F}(\omega) = f_1/|\omega|$, then (B.8) gives (for $\omega > 0$)

$$W(\tau, \omega) = \frac{f_1}{8\pi\gamma\frac{v}{c_o}}\Big(\frac{\gamma(1+\frac{v}{c_o})}{\omega} - \frac{\gamma(1-\frac{v}{c_o})}{\omega}\Big) = \frac{f_1}{4\pi\omega}.$$

This completes the proof of Proposition 2.

Appendix B.5. Proof of Proposition 3

We have

$$\left\langle U(\tau+\frac{\tau'}{2})U(\tau-\frac{\tau'}{2})\right\rangle = \int_{\mathbb{R}^3} \mathcal{A}(|\boldsymbol{k}|)\exp\left[i2\xi\sinh(\eta'/2)\big(|\boldsymbol{k}|\cosh(\eta)-k_z\sinh(\eta)\big)\right]d\boldsymbol{k},$$

with $\eta = c_o\tau/\xi$ and $\eta' = c_o\tau'/\xi$. After the change of variable $\boldsymbol{k}' = (k_x, k_y, k_z\cosh(\eta) - |\boldsymbol{k}|\sinh(\eta))$, we get

$$\left\langle U(\tau+\frac{\tau'}{2})U(\tau-\frac{\tau'}{2})\right\rangle = \int_{\mathbb{R}^3} \frac{\mathcal{A}(\mathcal{K}(\boldsymbol{k}',\eta))\mathcal{K}(\boldsymbol{k}',\eta)}{|\boldsymbol{k}'|}\exp\left[i2\xi\sinh(\eta'/2)|\boldsymbol{k}'|\right]d\boldsymbol{k}',$$

with

$$\mathcal{K}(\boldsymbol{k}',\eta) = \cosh(\eta)|\boldsymbol{k}'| + k_z'\sinh(\eta).$$

This function does not depend on η if and only if $k \mapsto \mathcal{A}(k)k$ is constant, if and only if $\hat{F}(\omega)$ is proportional to $|\omega|$ by (7). This completes the proof of Proposition 3.

Appendix B.6. Proof of Lemma 1

We address case 1 in order to compute $\Psi(v;a,b,c)$ defined by (28). We have

$$\frac{1}{a\cosh^2(s)+b\cosh(s)+c} = \frac{1}{a}\frac{1}{\cosh(s)-c_+}\frac{1}{\cosh(s)-c_-},$$

with

$$c_\pm = \frac{-b\pm\sqrt{\Delta}}{2a}, \quad \Delta = b^2-4ac.$$

We can check that $c_+ > 1$ (because $-c-a-b>0$) and $c_- < -1$ (because $-c-a+b>0$). We denote

$$x_\pm = \pm\text{argcosh}(c_+), \quad \tilde{x}_\pm = i\pi \pm \text{argcosh}(|c_-|), \quad \check{x}_\pm = 2i\pi + x_\pm.$$

We have $\cosh(x_\pm) = \cosh(\check{x}_\pm) = c_+$ and $\cosh(\tilde{x}_\pm) = -c_-$. We apply the residue theorem on the closed contour which is a rectangle $[-M,M]\cup[M,M+2i\pi]\cup[M+2i\pi,-M+2i\pi]\cup[-M+2i\pi,-M]$, with $M\to+\infty$. The contour contains two poles $\tilde{x}_\pm$ and it passes through four poles $x_\pm$ and $\check{x}_\pm$, so we get by the residue theorem:

$$\begin{aligned}\Psi(v;a,b,c)(1-e^{-2\pi v}) =& \frac{2i\pi}{a(c_+-c_-)}\Big\{\frac{1}{2}\frac{e^{ivx_-}}{\sinh(x_-)}+\frac{1}{2}\frac{e^{ivx_+}}{\sinh(x_+)}-\frac{e^{iv\tilde{x}_+}}{\sinh(\tilde{x}_+)}\\ &-\frac{e^{iv\tilde{x}_-}}{\sinh(\tilde{x}_-)}+\frac{1}{2}\frac{e^{iv\check{x}_+}}{\sinh(\check{x}_+)}+\frac{1}{2}\frac{e^{iv\check{x}_-}}{\sinh(\check{x}_-)}\Big\},\end{aligned}$$

which gives the desired result (29) using $\sinh(x_\pm) = \pm\sqrt{c_+^2-1}$, $\sinh(\tilde{x}_\pm) = \mp\sqrt{c_-^2-1}$, $\sinh(\check{x}_\pm) = \pm\sqrt{c_+^2-1}$, and $a(c_+-c_-) = \sqrt{\Delta}$.

Next we address case 2. We have

$$\Psi(v;0,b,c)=\frac{1}{b}\int_{\mathbb{R}}\frac{\exp(ivs)}{\cosh(s)+c'}ds,$$

with $c'=c/b>1$. We denote $x_\pm=i\pi+\text{argcosh}(c')$. We have $\cosh(x_\pm)+c'=0$. We apply the residue theorem on the contour $[-M,M]\cup[M,M+2i\pi]\cup[M+2i\pi,-M+2i\pi]\cup[-M+2i\pi,-M]$, with $M\to+\infty$, which contains the two poles $x_\pm$, and we get

$$\Psi(v;0,b,c)(1-e^{-2\pi v})=\frac{2i\pi}{b}\Big\{\frac{e^{ivx_+}}{\sinh(x_+)}+\frac{e^{ivx_-}}{\sinh(x_-)}\Big\},$$

which gives the desired result (30).

Finally we address case 3. We have

$$\Psi(v;a,0,c)=\frac{1}{a}\int_{\mathbb{R}}\frac{\exp(i(v/2)s)}{\cosh(s)+c'}ds$$

with $c'=1+2c/a<-1$. We denote $x_\pm=\pm\text{argcosh}(|c'|)$ and $\tilde{x}_\pm=2i\pi+x_\pm$. We have $\cosh(x_\pm)+c'=\cosh(\tilde{x}_\pm)+c'=0$. We apply the residue theorem on the contour $[-M,M]\cup[M,M+2i\pi]\cup[M+2i\pi,-M+2i\pi]\cup[-M+2i\pi,-M]$, with $M\to+\infty$, which passes through the four poles $x_\pm$ and $\tilde{x}_\pm$, and we get

$$\Psi(v;a,0,c)(1-e^{-\pi v})=\frac{i\pi}{a}\Big\{\frac{e^{i(v/2)x_+}}{\sinh(x_+)}+\frac{e^{i(v/2)x_-}}{\sinh(x_-)}+\frac{e^{i(v/2)\tilde{x}_+}}{\sinh(x_+)}+\frac{e^{i(v/2)\tilde{x}_-}}{\sinh(x_-)}\Big\},$$

which gives the desired result (31) with $\text{argcosh}(|c'|))=2\text{argcosh}(\sqrt{-c/a})$.

References

[1] H. Ammari, J. Garnier, W. Jing, H. Kang, M. Lim, K. Sølna, and H. Wang, Mathematical and Statistical Methods for Multistatic Imaging, Lecture Notes in Mathematics, Vol. 2098, Springer, Berlin, 2013. 16

[2] M. Antoniou, Z. Zeng, L. Feifeng, and M. Cherniakov, Experimental demonstration of passive BSAR imaging using navigation satellites and a fixed receiver, IEEE Geoscience and Remote Sensing Letters **9**, 477–481 (2012). 2

[3] T. H. Boyer, Thermal effects of acceleration through random classical radiation, Phys. Rev. D **21**, 2137–2148 (1980). 2, 3, 4, 6, 7, 21

[4] T. H. Boyer, Thermal effects of acceleration for a classical dipole oscillator in classical electromagnetic zero-point radiation, Phys. Rev. D **29**, 1089–1094 (1984). 6

[5] M. Cheney, A mathematical tutorial on synthetic aperture radar, SIAM Review **43**, 301–312 (2001). 2

[6] L. C. B. Crispino, A. Higuchi, and G. E. A. Matsas, The Unruh effect and its applications, Reviews of Modern Physics **80**, 787–838 (2008). 2

[7] J. C. Curlander and R. N. McDonough, *Synthetic aperture radar*, Wiley, New York, 1991. 2

[8] A. Curtis, P. Gerstoft, H. Sato, R. Snieder, and K. Wapenaar, Seismic interferometry turning noise into signal, The Leading Edge **25**, 1082–1092 (2006). 2, 4

[9] D. Deutsch and P. Candelas, Boundary effects in quantum field theory, Phys. Rev. D **20**, 3063–3080 (1979). 18

[10] M. Fink and J. Garnier, Ambient noise correlation-based imaging with moving sensors, Inverse Problems and Imaging **11**, 477–500 (2017). 2
[11] J. Garnier and M. Fink, Super-resolution in time-reversal focusing on a moving source, Wave Motion **53**, 80–93 (2015). 2
[12] J. Garnier and G. Papanicolaou, Passive sensor imaging using cross correlations of noisy signals in a scattering medium, SIAM J. Imaging Sciences **2**, 396–437 (2009). 2
[13] J. Garnier and G. Papanicolaou, Passive synthetic aperture imaging, SIAM J. Imaging Sciences **8**, 2683–2705 (2015). 2
[14] J. Garnier and G. Papanicolaou, *Passive Imaging with Ambient Noise*, Cambridge University Press, Cambridge, 2016. 2, 3, 4, 20
[15] P. Gouédard, L. Stehly, F. Brenguier, M. Campillo, Y. Colin de Verdière, E. Larose, L. Margerin, P. Roux, F. J. Sanchez-Sesma, N. M. Shapiro, and R. L. Weaver, Cross-correlation of random fields: mathematical approach and applications, Geophysical Prospecting **56**, 375–393 (2008). 2
[16] I. S. Gradshteyn et I. M. Ryzhik, *Table of Integrals, Series, and Products*, Academic Press, San Diego, 1980. 21, 22
[17] U. Leonhardt, *Essential Quantum Optics: From Quantum Measurements to Black Holes*, Cambridge University Press, Cambridge, 2010. 2, 5
[18] U. Leonhardt, I. Griniasty, S. Wildeman, E. Fort, and M. Fink, Classical analog of the Unruh effect, Phys. Rev. A **98**, 022118 (2018). 2, 3
[19] W. Rindler, Kruskal space and the uniformly accelerated frame, Am. J. Phys. **34**, 1174–1178 (1966). 5
[20] M. Rodriguez-Cassola, S. V. Baumgartner, G. Krieger, and A. Moreira, Bistatic TerraSAR-X/F-SAR Spaceborne-Airborne SAR experiment: Description, data processing, and results, IEEE Transactions on Geoscience and Remote Sensing **48**, 781–794 (2010). 2
[21] C. Rovelli and M. Smerlak, Unruh effect without trans-horizon entanglement, Phys. Rev. D **85**, 124055 (2012). 16
[22] S. M. Rytov, Theory of the Electric Fluctuations and Thermal Radiation [in Russian], Publication of Acad. of Sciences of USSR, Moscow (1953), English translation: Air Force Cambridge Research Center, Bedford, MA (1959). 2
[23] N. M. Shapiro, M. Campillo, L. Stehly, and M. H. Ritzwoller, High-resolution surface wave tomography from ambient noise, Science **307**, 1615–1618 (2005). 2
[24] W. G. Unruh, Notes on black-hole evaporation, Phys. Rev. D **14**, 870–892 (1976). 2, 6
[25] K. Wapenaar, D. Draganov, R. Snieder, X. Campman, and A. Verdel, Tutorial on seismic interferometry: Part 1 - Basic principles and applications, Geophysics **75**, A195–A209 (2010). 2